ASCOMP
MULTIPHASE FLOW SCIENCE AND TECHNOLOGY

TransAT Report Series

– Applications –

TransAT for Oil & Gas

On the Simulation of Subsea Oil Spill

Ascomp Switzerland

Edited by: Dr C. Narayanan

Release date: Sep, 2014.

References: TRS-A/ 06-2014

www.ascomp.ch - info@ascomp.ch

Table of Contents

Abstract:
This report describes the modeling and simulation technique recently developed within the code TransAT to predict deep-sea oil spill. The approach is deliberately placed beyond the simplified models used hitherto (e.g. cone model, integral model and plume model), in that it relies on solving the unsteady full Navier-Stokes equations in three dimensions in transient mode for a mixture of N-phases, and incorporates an additional equation for hydrate formation, fully coupled with the transport equations to cope with phase change. The model requires thermodynamics properties of the fluid be defined at the water level under consideration. We report first results of a deep-sea blowout in the form of a 3D jet for a specific type of oil.

1. Introduction

Hazardous gas hydrate formation and release may cause blockages in oil production lines, and as such it remains today one of the main concerns to deepwater field developments. The present strategy of operators is commonly focused on the deployment of prevention methods that aim at producing outside the hydrate domain. This can mainly be achieved via pipeline insulation (for oil dominated systems) or thermodynamic chemical injection (for gas dominated systems). Another strategy is to produce inside the hydrate domain by transporting the hydrate phase as slurry of hydrate particles dispersed in the oil phase, a strategy first proposed about two decades ago [1] and led to developments of Anti-Agglomerant additives (AA), a family of the so-called Low Dosage Hydrate Inhibitors (LDHI) [2-5]. Even so, injection of such chemicals remains still marginal. Similarly, natural surfactants (asphaltenes, resins, acidic compounds, etc.) present in most of black oils were also considered as potential agents enabling hydrates to be transported as a slurry [6]. Operators have been envisaged to take advantage of such surfactant properties, particularly to ensure restarting after a long shutdown. Associated with subsea water separation, oil properties would also make viable the development of satellite fields connected to existing platforms via long tie-backs.

Investigations of crude oils with respect to hydrate control have thus been conducted for numerous years [7-9]. Most of them show results on plugging or non-plugging occurrence in laboratory facilities or pilot loops and do not allow us to predict flow conditions inside the hydrate domain [10-11].

In terms of simulation, 1D models for hydrate-plug formation in flowlines are available, and have been successfully applied for subsea tiebacks [12]. 3D predictions are however rare, and, only CFD codes like Star-CD [13] and TransAT [14] have shown validated predictive capabilities applied to real flowline plugging problems.

2. State of The Art

The simulation of deep-sea dispersion has gone through successive eras, with an increasing degree of complexity (see the review of Riew et al. [12]). Early models propose the so-called Cone Modeling approach, whereby the bubbly jet is assumed to disperse laterally as a cone of angle θ, in a monotonic, linear way from sea bed to surface. The model consists in providing a linear relationship linking the jet spread rate $b(z)$ to the spreading angle θ (the model is illustrated in Fig. 1, left panel): i.e. $b(z)= z \tan(\theta/2)$. Needless to say that the values of the model constants vary significantly; e.g. the cone angle could vary – depending on the experiment- between 10 and 23 Degrees. Integral models developed later propose another more elaborate approach based on momentum integration along the jet trajectory and using hypotheses as to the dimensionality of the flow. The general formulation as proposed by Fazal and Milgram [13] serves as a good basis to describe the model: briefly, it consists

in assuming that the mean fluid velocity and mean density defect obey Gaussian distributions. The theory makes use of the isothermal expansion law relating the gas density to the water depth via the hydrostatic pressure.

To close the system of conservation equations for the plume, three algebraic expressions are solved: the conservation of liquid and gas fractions, together with the conservation of momentum. These expressions are then combined together yielding a system of PDE (only derivatives in z) which can be solved numerically using any simple iterative approach. The final outcome consists of: centerline gas fraction and liquid velocity, S(z) and U(z), together with the plume width, b(z). The Plume Model has been used for a decade at least, with more sophisticated models as to the pertinent physics (e.g. hydrate formation) albeit it retains the similar integration lines like the Integral Model [12].

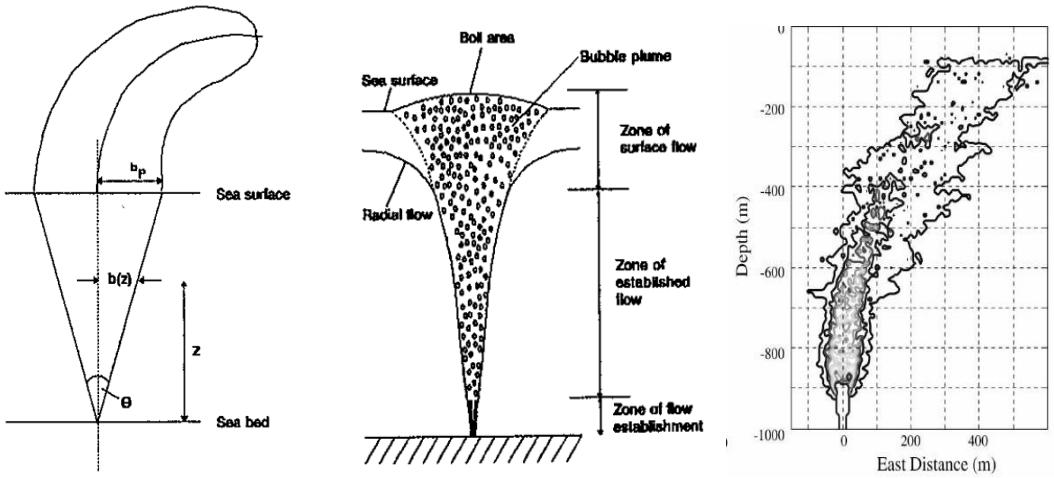

Figure 1: Sketch of Cone Models, Integral Models and Plume Models (Riew et al. [12]).

3. Example 2: macroscale phase separation (hydrate formation below sea)

This example shows rather what is possible today with a CFD code like TransAT to predict the formation of hydrates under very stiff thermodynamics conditions. The test case relates to the formation of hydrates under deep sea: below 1000m. This problem came to be known to the public through the Oil Spill disaster in the Gulf of Mexico (July 2010). In contrast to the previous problem, where the phase separation occurs at very small scales and has been treated using the phase field theory, here the problem requires the use of a phase-averaged approach since the length scale of the problem is huge.

Under 1000 meter, water temperature is in the temperature range of -1°C to 6°C, pressure is close to 100 bar, which helps the formation of hydrates. The problem amounts at 5 phases: oil light components C1, oil heavy components C2, gas, water and hydrates. To solve the problem we had to use the N-phase homogeneous model with Algebraic Slip, where drift is considered between each phase. The thermodynamics is also included, e.g. variable material properties with temperature and pressure, rheology of oil using some constitutive laws, etc. The problem, though far off from our objectives, actually shows that it can be applied to CO2 dissolution into cold-pressurized water systems, as for refrigeration. And this is exactly what we would like to pursue in this project.

3.1 Transport Equations

The N-phase model based on the mixture algebraic slip approach is used here, which amounts at solving the following equations [14-15]:

$$\frac{\partial \rho_m}{\partial t} + \frac{\partial}{\partial x_j}\left(\rho_m u_{m_j}\right) = 0$$

$$\frac{\partial \rho_k \alpha_k}{\partial t} + \frac{\partial}{\partial x_j}\left(\rho_k \alpha_k (u_{m_j} + u^D_{k,j})\right) = 0$$

$$\frac{\partial}{\partial t}\left(\rho_m u_{m_j}\right) + \frac{\partial}{\partial x_j}\left(\rho_m u_{m_i} u_{m_j} + \frac{\rho_m}{Y_L}\sum_k Y_k \overline{u^D_{k,i} u^D_{k,j}}\right) = \frac{\partial}{\partial x_j}\left[-p_m \delta_{ij} + \sigma_{m,ij}\right] + \frac{\partial}{\partial x_j}\left[2\alpha_G \mu_G \sigma^D_{k_{ij}} + 2\alpha_L \mu_L \sigma^D_{L_{ij}}\right] + \rho_m g \quad (1)$$

where the mixture velocity, density and drift velocity are defined by:

$$u_m = \sum \alpha_k \rho_k u_k \,/ \sum \alpha_k \rho_k; \quad \rho_m = \sum \alpha_k \rho_k; \quad Y_k = \alpha_k \rho_k \,/ \rho_m; \quad u^D_k = u_k - u_m \quad (2)$$

These equations are solved for 'k' phases present simultaneously in the system, sharing a common pressure field p_m, with a drift velocity u_D and associated stresses in the momentum equations prescribed algebraically between the phases, using [15]:

$$u_{D_j} = \frac{2}{9}\frac{\alpha_L R_b^2 (\rho_G - \rho_L)}{\alpha_G \mu_m} Y_L (Y_L - \alpha_L)\frac{\partial p}{\partial x_j} + HoT \quad (3)$$

3.2 Jet Instability

The jet is expected to oscillate in three dimensions, exhibiting large scale motions (meandering around its axis) on which smaller scale motions are superimposed. It is unlikely that normal uniform inflow conditions would mimic the inherent unstable behavior, regardless of the degree of sophistication of turbulence modeling and simulation adopted. This was indeed carefully considered in this work, leading to the conclusion that inflow conditions of the jet should be perturbed using some analytical formulation, introducing both a main symmetrical mode:

$$V_x(y,z) = V_0 \; f(y,z); \quad f(y,z) = \sec h\left(\frac{\sqrt{y^2+z^2}}{a}\right)^m \quad (4)$$

and additional helical modes (up to 5th order taken here):

$$\begin{cases} V_y(x,y,z) = V_{y,0} \; f(y,z) + \dfrac{1}{n}\displaystyle\sum_{j=1,n} a_n \sin(jk_0 x + \phi_j) \\ V_z(x,y,z) = V_{z,0} \; f(y,z) + \dfrac{1}{n}\displaystyle\sum_{j=1,n} a_n \sin(jk_0 x + \phi_j) \\ V_{y,0} = (0.05 - 0.12)\, V_0 \end{cases} \quad (5)$$

Similar models with various modal functions, coefficients and main form f(y,z) have been proposed in the literatures [16-17], though none has been compared to real experiments, e.g. Simiano et al. [18].

3.3 Turbulence Modelling

The Reynolds number of this class of flows is clearly out of reach of LES, which should be the best way to reproduce the oscillatory behaviour of the jet. URANS would be useful, but the degree of flow unsteadiness expected is low compared to LES. The alternative that seems to be well suited for this category of flows is the VLES, short for Very Large-Eddy Simulation. VLES is based on the concept of filtering a larger part of turbulent fluctuations as compared to LES (as the name clearly implies). This directly implies the use of a more elaborate sub-grid modelling strategy than a zero-equation model like in LES. The VLES implemented in TransAT is based on the use of k-ε model as a sub-filter model. The filter width is no longer related to the grid size; instead it is made proportional to a characteristics length-scale (Λ) that is larger than the grid size (~ Δx), but necessarily smaller than the macro length-scale of the flow. Increasing the filter width beyond the largest length scales will lead to predictions similar to RANS, whereas in the limit of a small filter-width the model predictions should tend towards LES.

VLES could thus be understood as a natural link between conventional LES and URANS. If the filter width is smaller than the length scale of turbulence provided by the RANS model, then larger turbulent flow structures will be able to develop during the simulation, provided that the grid resolution and simulation parameters are adequately set. For a more detailed presentation and a discussion on the values of the model constants, the reader can refer to [19-20]. One of the key hypotheses in VLES is that the Kolmogorov equilibrium spectrum is supposed to apply to the sub-filter flow portion, which allows defining the eddy viscosity for the sub-filter flow as follows:

$$\nu_t = C_\mu \frac{k^2}{\varepsilon} C_3 \frac{\Delta\varepsilon}{k^{3/2}} \; f(\Delta, k, \varepsilon); \quad with \quad f(\Delta, k, \varepsilon) = \min\left|1, \quad C_3 \Delta\, \varepsilon / k^{3/2}\right| \tag{6}$$

where $f(\Delta, k, \varepsilon)$ is a length-scale limiting function, introduced by Johansen et al. [20].

3.4 Rheology Modelling

The rheology of hydrates has been included in TransAT via two models that consider an apparent viscosity of the mixture: Ishii and Zuber [21] (also revised by Ishii and Mishima) and Colombel et al. [22] more recent variant. In the first model, which is the mostly used one, the apparent viscosity is defined using this expression:

$$\mu_m = \mu_c \left(1 - \frac{\phi_p}{\phi_{pm}}\right)^{-2.5\phi_{pm}\mu^*} \tag{8}$$

where ϕ_{pm} is the concentration for maximum packing, which for solid particles is equal to 4/7. For solid particles, μ*= 1, whereas for bubbles and droplets, it takes the form:

$$\mu^* = \frac{\mu_p + 0.4\mu_c}{\mu_p + \mu_c}$$

Colombels' [22] model, however, accounts in addition for two mechanisms of agglomeration: the first one is the contact-induced agglomeration mechanism, for which the crystallization-agglomeration process is described as the result of the contact between a water droplet and a hydrate particle. The second one is the shear-limited agglomeration mechanism for which the balance between hydrodynamic force and adhesive force is considered. In summary, in this extended model, the viscosity of the suspension is made proportional to the effective volume fraction ϕ_{eff}:

$$\mu = \mu_0 \frac{1-\phi_{eff}}{\left(1-\frac{\phi_{eff}}{\phi_M}\right)^2} \tag{8}$$

with μ_0 being the oil viscosity and ϕ_M the maximum packing. The effective volume fraction scales with the actual volume fraction ϕ (≈ water cut) as follows:

$$\phi_{eff} = \phi\left(\frac{\tau_0}{\tau}\right)^{(3-m)D} \tag{9}$$

3.5 Hydrate Kinetics & Formation

The formation of hydrates here is from two distinct sources:

- Gas + water → hydrates,
- C1 + water → hydrates.

To complete the model (Eqs. 1-3 above), an additional transport equation for the hydrates is introduced (referring to its concentration per unit volume),

$$\frac{\partial \rho_c C}{\partial t} + \frac{\partial}{\partial x_j}\left(\rho_c u_j C\right) = \frac{\partial}{\partial x_j}\left[D_c \frac{\partial C}{\partial x_j}\right] + S_h \tag{10}$$

The last term in the RHS denotes the source/sink for hydrates; formation or dissolution, defined based on thermodynamics properties, and is directly linked to the mass transfer rate defined in the equation below (11). The dissolution is not to be taken into account at deep water levels, but when the free surface is approached, Further, another hypothesis should be made whether the hydrates form in a very fast way, or, in contrast, there is a time delay during which crystals form, and as such a hydrates kinetics equation has to be solved in parallel to estimate the rate of mass transfer, i.e. [23-25]:

$$\frac{dn}{dt} = A a_s \exp\left(\frac{\Delta E}{RT}\right)\exp\left(-\frac{a_s}{\left[T-T_{eq}\right]^{\theta}}\right)P^{\gamma} \tag{11}$$

As stated above the dissolution of hydrates should be accounted for only as the water surface is approached, as suggested by the hydrate phase-equilibrium diagrams of both CH4 and natural gas at some location in the Gulf of Mexico shown in Fig (2) below:

The figure shows that phase inversion occurs at about 600m below sea for methane and at 450m for natural gas. This means that dissolution of methane should not be considered when the model is applied near the sea bed.

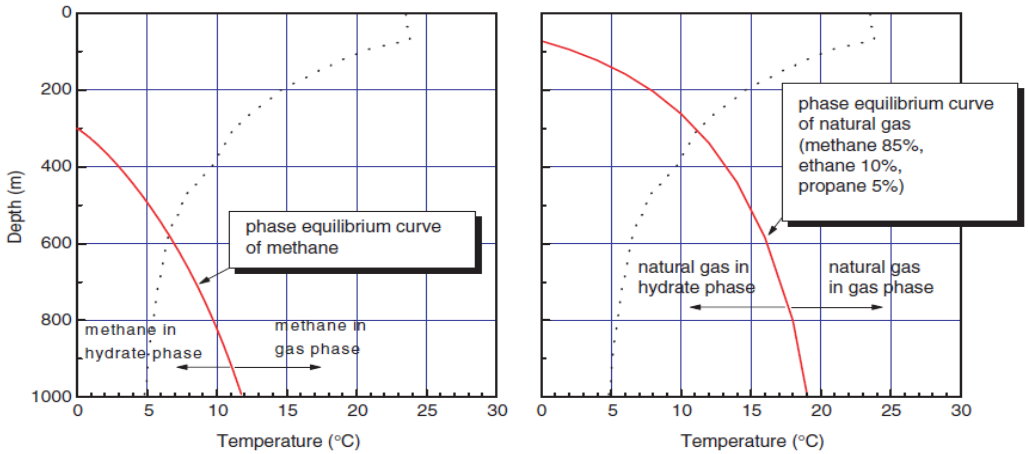

Figure 2: Hydrate phase-equilibrium diagrams of CH4 (left) and natural gas (right) superimposed on temperature distribution at some location in the Gulf of Mexico Grid (taken from Yapa et al., 2005).

3.6 Hydrate wall-adhesion modelling

One of the key issues in modeling hydrate plugging of flowlines is to consider whether the hydrates formed stick (adhere) to the solid wall or not. Further, it is unclear which of the hydrates do really stick: the one formed by methane phase change in contact with cold water, or those formed by the light components of oil (C1-C9) changing phase. For the purpose, several models have been developed and implemented in code TransAT, one of which is based on the stability principle of the hydrates in contact with the walls, combined with an advanced rheology model similar properties to Bingham's model. Of course, this model does not apply to the free jet flow considered, but it has been used to predict the plugging in the canopy employed by BP to collect the oil in the aftermath of the blow up. Results are confidential and cannot be shown here.

3.7 Selected Results

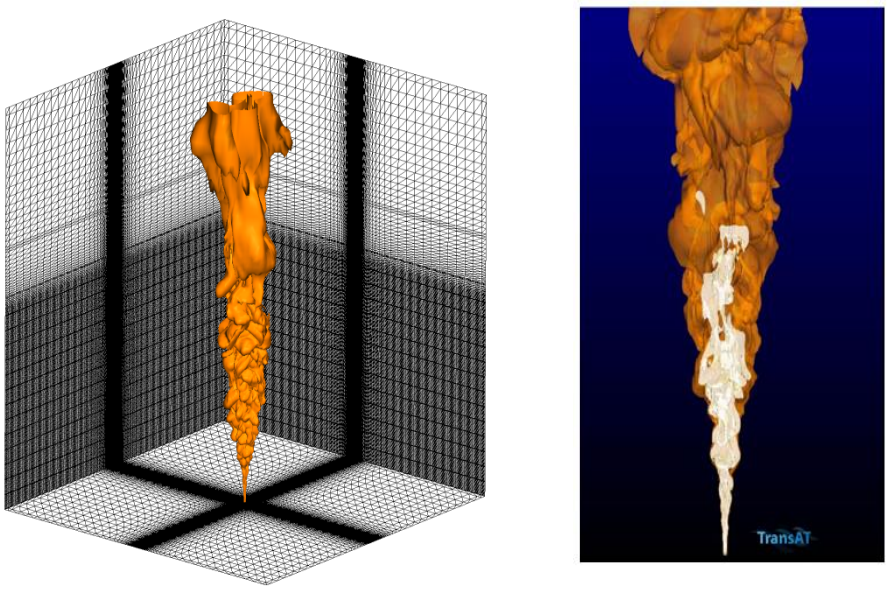

Figure 3: Grid, computational domain and deep sea jet. Beginning of gas injection (gas colour is brown; white colour represents hydrates). Hydrates formed immediately after gas injection.

Figure 3 (left panel) shows the computational grid (consisting of 5 mill. Cells refined along the jet centerline in particular) and the multiphase flow jet. The inflow conditions follow the prescriptions in Eqs. (4-5), with a mass flow rate of 40.000 Brl/Day. Symmetry conditions were employed in the lateral planes, and pressure boundary conditions on the top. VLES has been applied for turbulence, together with rheology model of Palermo. Thermodynamics properties of the material were delivered. Clearly, the refined grid near the bottom is capable to reproduce the details of the oscillation of the jet, while further up towards the free surface, the grid resolution captures only the very large scale deformations. The early stage of hydrate formation in the 3D unsteady jet is shown in the right panel (colored in white). Overall the unsteady behavior of the jet is very well predicted, exhibiting various modes and interface deformations.

Figure 4 below shows snapshots at t = 72 and 210 seconds of the main constituents of the flow: i.e. gas, hydrates, oil light and oil heavy. The water phase is colored in blue. The gas and oil light components change phase immediately upstream the leakage, at about 10m: the oil heavy and hydrates exhibit a dispersive behavior mainly driven by turbulence, above the limit of 10m. Figure 4 presents cross-sectional contours of hydrates, instantaneous and time average, at three different elevations. While the instantaneous pictures reveal a strong dispersion with turbulence, in particular for the upper two locations, the time average panels show a sort of annulus, whereby the higher hydrate concentrations are centered. This is due to the water being drifted by entrainment effects towards the centerline of the jet, which is best illustrated when looking at the instantaneous pictures depicted in Fig. 5. Such a behavior is unlikely to be predicted by steady state simulations; the results show the importance of predicting the unsteady features (large and small scales) of turbulence with which the different phases interact and get distributed in the domain.

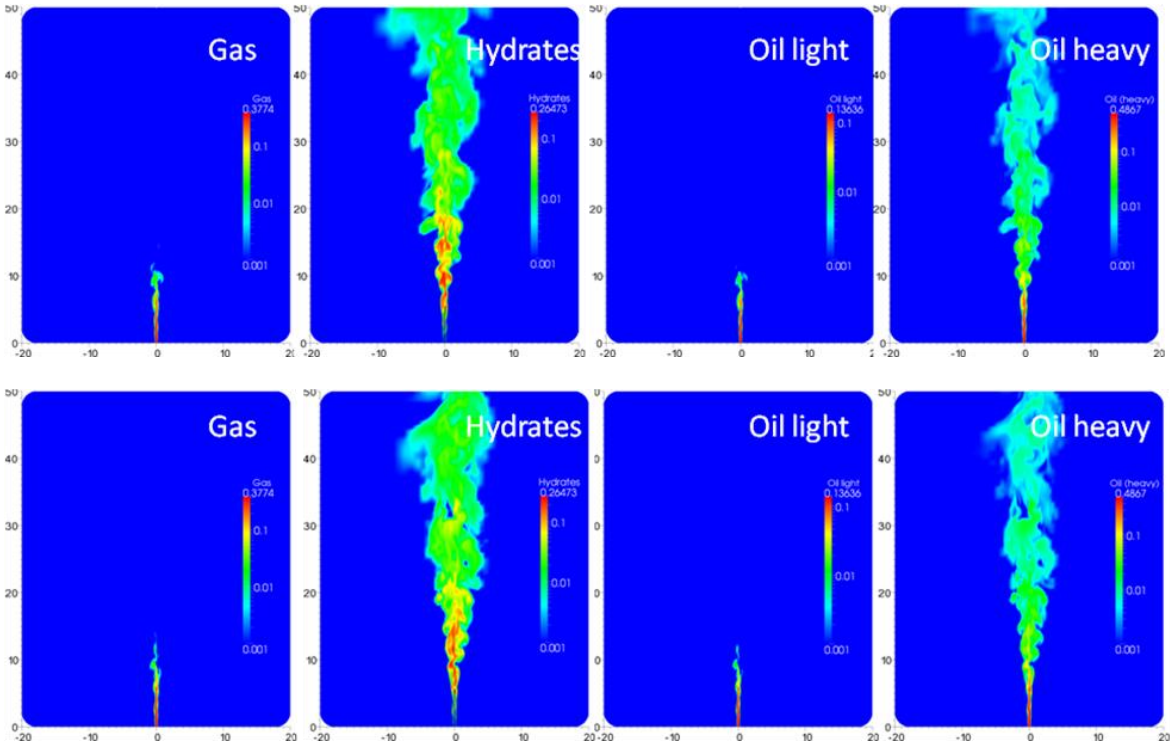

Figure 4: Transient snapshots at 75 and 210 s of simulation time.

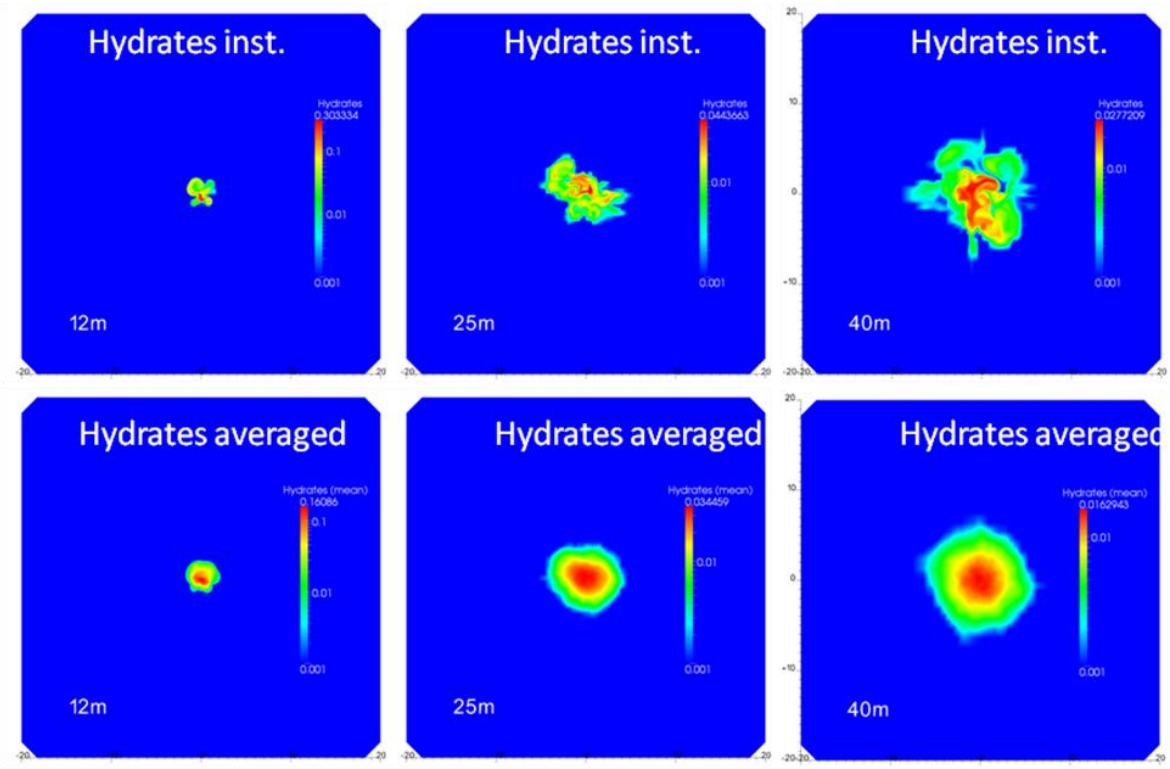

Figure 5: Transient and time-averaged cross-flow snapshots of the hydrate contours.

4. Conclusions

Three-dimensional, unsteady simulations of oil spill at 1000m below sea level were performed using the CMFD code TransAT. The model is more sophisticated than earlier Cone Models, Integral Models and Plume Models, which ignore the critical issue in the problem: that is the transient interaction of the constituents with the surrounding turbulence. Because the Reynolds number of the flow is very high, resort was made to the VLES approach to model the subscales of turbulence. The simulation results reveal that the model is capable to predict the three basic sequences about the hydrate formation process: the mixing of the gas phase with the water phase; the diffusion through the liquid film to the hydrate-liquid interface; and the reaction of gas with the aqueous phase (Nucleation and Crystallization of CO2 hydrates), which has been lumped using a concentration equation with a rate of phase change coarse-grained from a hydrates kinetics equation. Simulation results have shown rapid and continuous dissolution of gas and light oil components into hydrates within a tiny region of space, not exceeding 10m from sea bed.

Of course there have been a certain number of simplifications to the problem, e.g., reduction of the number of oil components and neglecting their interactions. To complete the model, the rheology of the oil components and hydrates has to be revisited; probably not requiring a kinetics equation, the dissolution of hydrates may be taken into account if the domain extends to subsea level close to the surface, in which case other models [26-27] have to be implemented as well.

References

1. Sugier A., Bourgmayer P., Behar E., Freund E. (1990) Method of Transporting a hydrate Forming Fluid, US Patent 4,915,176.
2. Behar E., Delion A.S., Sugier A., Thomas M. (1994) Plugging control of production facilities by hydrates, Ann. N.Y. Acad. Sci. 715.
3. Palermo T., Sinquin A., Dhulesia H., Fourest J.M. (1997) Pilot loop tests of new additives preventing hydrate plugs formation, Multiphase'97, 7th International Conference on Multiphase, Cannes, 1997, pp. 133-147.
4. Palermo T., Maurel P. (1999) Investigation of hydrates formation and hydrates transportation with and without dispersant additives under multiphase flow conditions, Multiphase'99, 9th International Conference on Multiphase, Cannes, 1999, pp. 567-582.
5. Mehta A.P., Herbert P.B., Cadena E.R., Weatherman J.P. (2002) Fulfilling the Promise of Low Dosage Hydrate Inhibitors: Journey from Academic Curiosity to Successful Field Implementation, OTC 14057, Houston, Texas, 6-9 May 2002.
6. Palermo T., Mussumeci A., Leporcher E. (2004) Could Hydrate Plugging Be Avoided Because of Surfactant Properties of the Crude and Appropriate Flow Conditions? OTC 16681, Houston, Texas, 3-6 May 2004.
7. Nygaard N.F. (1989) Transportability of Hydrates in Multiphase Systems, Proceedings of the 4th International Conference on Multi-Phase Flow, Nice, June, 1989.
8. Maurel P., Palermo T., Hurtevent C., Peytavy J.L. (2002) Shutdown/Restart tests with an acidic crude under hydrate formation conditions for a deepwater development, Proceedings of the 13th International Oil Field Chemistry Symposium, Geilo, Norway, 17-20 March 2002.
9. Palermo T., Camargo R., Maurel P., Peytavy J.L. (2003) Shutdown/Restart pilot loop tests with an asphaltenic crude under hydrate formation conditions, Multiphase 03, 11th International Conference on Multiphase 03, San Remo, pp. 219-237.
10. Camargo R., Palermo T. (2002) Rheological properties of hydrate suspensions in an asphaltenic rude oil, Proceedings of the 4th International Conference on Gas Hydrates, 19-23 May 2002, Yokohama Symposia, Yokohama, Japan.
11. Mills P. (1989) Non-Newtonian behaviour of flocculated suspensions, J. Phys. Lett. 46, L301-L309.
12. Riew P.J, Ghallagher P., Hughes D.M. (1995) Dispersion of subsea releases, HSE Books, Offshore Technology Report OTH 95-465
13. Davies R.S. et al., (2009) Prediction hydrate-plug formation in a subsea tieback, SEP Production & Operations, 573-578.
14. Lo S. (2011) CFD modelling of hydrate formation oil-dominated flows, OTC21509, Offshore Technology Conference Houston Texas, 2-5 May 2011.
15. Fazal R., Milgram J.H. (1980) The structure of gas-liquid plumes above blowouts, MIT Report 0380-12, 1980.
16. Drew, D.A. and Passman, S.L (1998) Theory of multicomoponent fluids, Springer, New York.
17. Mannin M., Taivassalo V. (1996) On the mixture model for multiphase flow, VTT Pubs. 288.
18. Lesshafft L., Huerre P., Sagaut P. (2005) Frequency selection in globally unstable thin shear layer jets. Physics of Fluids, 19 (054108).
19. Oparin S., Abarzhi A. (1999) Three-dimensional bubbles in Rayleigh–Taylor instability, Phys. Fluids, 11, pp. 3306-3311.
20. Simiano M., Lakehal D., Lance M., Yadigaroglu G. (2009) Turbulent transport mechanisms in oscillating bubbly plumes, J. Fluid Mech., 633, 191231

21. Labois M., Lakehal D., (2011) Very-Large Eddy Simulation (V-LES) of the Flow across a Tube Bundle, (available online: DOI: 10.1016/j.nucengdes.2011.02.009), Nucl. Eng. Design.
22. Johansen S.T., Wu J., Shyy W. (2004) Filtered-based unsteady RANS computations, Int. J. Heat & Fluid Flow, 25, pp. 10-21.
23. Ishii, M., Zuber, N. (1979) Drag coefficient and relative velocity in bubbly, droplet and particulate flow. AIChE J. 25, pp. 843-854.
24. Colombel, P. Gateau, L. Barré, F. Gruy and T. Palermo, (2009) Discussion of Agglomeration Mechanisms between Hydrate Particles in Water in Oil Emulsions, Oil & Gas Science and Technology – Rev. IFP, 64, pp. 629-636
25. Vysniauskas A., Bishnoi, P.R. (1983) A kinetic study of Methane hydrate formation, Chemical Engineering Science 38(7), pp. 1061-1072
26. Englezos, P., Kalogerakis, N., Dholabhai, P.D., Bishnoi, P.R. (1987) Kinetics of formation of Methane and Ethane gas hydrates, Chemical Engineering Science 42(11), pp. 2647-2658.
27. Zheng L., Yapa P.D., Chen F. (2002) A model for simulating deepwater oil and gas blowouts Part I: Theory and model formulation, J. of Hydraulic Research 41(4), pp. 339-351
28. Riestenberg D.E., West O.R., Lee, S.-Y., McCallum S. D., Phelps T. J. (2003) Sediment Surface Effects on Methane Hydrate Formation and Dissociation. Marine Geology, 198, pp. 181-190.
29. Zatsepina O.Y., Riestenberg D.E., McCallum, S.P., Gborigi M., Brandt C., Buffett B.A., Phelps T. J. (2004) Influence of Water Thermal History and Overpressure on CO2-Hydrate Nucleation and Morphology. American Mineralogist, 89, pp. 1254-1259.